ROYAL SOCIETY OPEN SCIENCE

rsos.royalsocietypublishing.org

Research

Cite this article: Liu Y, Zhu C-l, Zheng X-y, Qin L-l, Yang S-x, Liu Z-q. 2018 Phase transition and switchable dielectric behaviours in an organic–inorganic hybrid compound: (3-nitroanilinium)$_2$(18-crown-6)$_2$(H_2PO_4)$_2$(H_3PO_4)$_3$(H_2O). *R. Soc. open sci.* **5**: 180738.
http://dx.doi.org/10.1098/rsos.180738

Received: 24 May 2018
Accepted: 29 August 2018

Subject Category:
Chemistry

Subject Areas:
supramolecular chemistry

Keywords:
crystal structure, structure phase transition, dielectric anisotropy, pendulum-like motion, three-dimensional layer

Author for correspondence:
Zun-qi Liu
e-mail: zunqi85@163.com

This article has been edited by the Royal Society of Chemistry, including the commissioning, peer review process and editorial aspects up to the point of acceptance.

Electronic supplementary material is available online at https://dx.doi.org/10.6084/m9.figshare.c.4238654.

THE ROYAL SOCIETY PUBLISHING

Phase transition and switchable dielectric behaviours in an organic–inorganic hybrid compound: (3-nitroanilinium)$_2$(18-crown-6)$_2$(H_2PO_4)$_2$(H_3PO_4)$_3$(H_2O)

Yang Liu, Chun-li Zhu, Xiao-yuan Zheng, Liu-lei Qin, Shuang-xi Yang and Zun-qi Liu

Chemical Engineering College, Xinjiang Agricultural University, Urumqi 830052, People's Republic of China

Y-qL, 0000-0001-6096-7166

An organic–inorganic hybrid compound with an extensive three-dimensional (3D) crystal structure, (3-nitroanilinium)$_2$(18-crown-6)$_2$(H_2PO_4)$_2$(H_3PO_4)$_3$(H_2O) (**1**), was synthesized under slow evaporation conditions. Differential scanning calorimetry measurements indicated that **1** underwent a reversible phase transition at *ca* 231 K with a hysteresis width of 10 K. Variable-temperature X-ray single-crystal diffraction revealed that the phase transition of **1** can be ascribed to coupling of pendulum-like motions of its nitro group with proton transfer in O–H···O hydrogen bonds of the 3D framework. The temperature dependence of its dielectric permittivity demonstrated a step-like change in the range of 150–280 K with remarkable dielectric anisotropy, making **1** a promising switchable dielectric material. Potential energy calculations further supported the possibility of dynamic motion of the cationic nitro group. Overall, our findings may inspire the development of other switchable dielectric phase transition materials by introducing inorganic anions into organic–inorganic hybrid systems.

1. Introduction

Phase transition compounds with electric, magnetic, and thermally switchable ON/OFF states usually provide an efficient strategy for the design of multifunctional switching materials such as ferroelectrics [1–9]. Generally, such physical responses always exhibit abrupt changes in the vicinity of a

phase transition, giving rise to phase transition materials with potential applications in energy storage, temperature controlling, data communications and phase shifters [10–19]. Molecular switchable dielectrics typically have dielectric constants that vary between high and low states upon temperature change. For this reason, they are one of the most attractive and promising phase transition materials for application in modern multifunctional materials [20–26]. In this regard, organic–inorganic hybrid compounds that combine desirable characteristics from both types of constituents, especially those that can be prepared into large-size crystals, may be an effective strategy for obtaining ideal phase transition materials [27–33].

Several novel organic–inorganic hybrid phase transition materials with electrical switches have been synthesized [34–38]. Previous studies have also demonstrated that freezing and reorientation of the organic cations and deformation of the anionic framework can easily induce phase transitions. To obtain molecular crystals that exhibit such phase transitions, complexes based on crown ether and its derivatives have recently been investigated [39–46]. These materials are crucial not only because they comprise diverse molecule motions, thereby providing favourable conditions for reversible phase transitions; but also for their extensive utilization in supramolecular chemistry and crystal engineering for assembling multiple ionic compounds to produce an assortment of host–guest molecules [47–49]. Tang *et al*. successfully demonstrated a class of perovskite structure clathrates, [Hcpa-(18-crown-6)]$^{+}$[ClO_4]$^{-}$, where Hcpa represents the protonated cyclopentylamine cation, that display unusual multisequential reversible phase transitions accompanied by switchable dielectric behaviour. Sequential reversible phase transitions and symmetry breaking occurs in response to the stepwise synergistic disordering of the Hcpa cations and ClO_4^- anions. Shi and co-workers reported the supramolecular phase change material (PCM) potassium hydrogen bis(dichloroacetate)-18-crown-6, which undergoes a reversible second-order phase transition at 181.8 K (*T*c). The phase transition was ascribed to order–disorder transformations of pendulum-like motions of the $CHCl_2COO$/$CHCl_2COOH$ units between the low- and room-temperature phases [50–52].

We have previously reported molecular rotators based on supramolecules formed by crown ether and anilinium derivatives that showed reversible phase transitions via hydrogen bonding. For example, a layered crystal of (2-nitroanilinium)(18-crown-6)(IO_4) showed a pair of reversible peaks at 260.5 K (cooling) and 264.5 K (heating) with heat hysteresis of approximately 4 K. Structural analysis and potential energy calculations indicated that the dielectric anomaly and phase transition occur because of intra- and intermolecular proton transfer of $-NH_3^+$ in 2-nitroanilinium as a consequence of $-NO_2$ motion in the cation [53–55]. It was suggested that hydrogen-bonding interactions and/or molecular motion give rise to symmetry breaking, thus leading to the dielectric anomaly behaviour as well as the phase transition. With a view to expand this research, a protonated 3-nitroanilinium cation that can form supramolecular rotator structures with 18-crown-6 through hydrogen-bonding interactions was adopted as a new type of molecular phase transition material. Compared with 2-nitroanilinium, 3-nitroanilinium provides a larger volume for molecular motion within the crystal, thereby reducing the potential energy required for molecular motion. Meanwhile, $H_2PO_4^-$ is used as the counter-ion in the supramolecular cation assembly. By providing active H atoms, $H_2PO_4^-$ easily forms hydrogen-bonding interactions that greatly contribute to the phase transition behaviour and dielectric and ferroelectric properties of the material. In this study, we successfully synthesized a new organic–inorganic hybrid compound, (3-nitroanilinium)$_2$(18-crown-6)$_2$(H_2PO_4)$_2$(H_3PO_4)$_3$(H_2O) (**1**), which not only shows sequential reversible structure phase transition at *ca* 231 K, but also exhibits switchable dielectric anisotropy behaviour along the *a*-, *b*- and *c*-axes. The molecular motions are discussed in terms of X-ray crystallographic analyses and potential energy calculations.

2. Experimental

2.1. Material and methods

All reagent-grade chemicals and solvents were of analytical grade and used without any further purification. The IR spectra of compound **1** were recorded on an Affinity-1 spectrophotometer (400–4000 cm^{-1}) at room temperature, with all samples prepared as diluted KBr pellets (electronic supplementary material, figure S1). Elemental analysis was carried out on a Vario EL Elementar Analysen systeme GmbH at the Collaboration Center of TRW Research, Shandong. Thermogravimetric analysis (TG) and differential thermal analysis (DTA) measurements were performed on a TA Q50 instrument under flowing nitrogen at a heating rate of 10 K min^{-1}. Differential scanning calorimetry

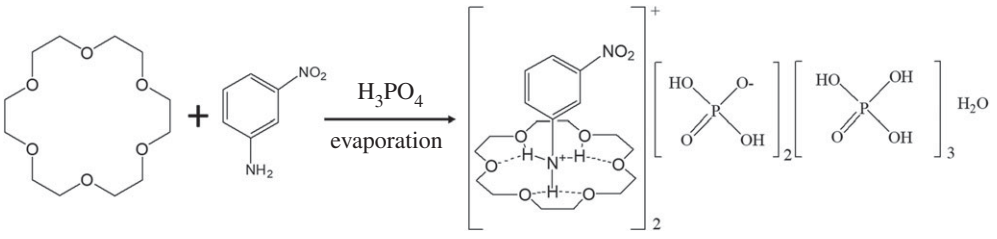

Scheme 1. Synthesis of compound **1**.

(DSC) measurements were performed on a TA Q2000 DSC instrument by heating and cooling the crystal samples (12.3 mg) at a rate of 10 K min^{-1} within the temperature range of 210–260 K under nitrogen at atmospheric pressure. Single crystals of **1** deposited with a silver conducting glue were used for the dielectric measurements.

2.2. Preparation of **1**

The title compound **1** was prepared by slow evaporation of a mixture solution at room temperature, as shown in scheme 1. An acetonitrile solution (20 ml) of 3-nitroaniline (1.4 mol, 0.208 g) was added slowly to an acetonitrile solution (20 ml) of 18-crown-6 (1.4 mol, 0.400 g), followed by the dropwise addition of 0.174 g phosphoric acid (85%). The solvent was evaporated for five days at room temperature to give a block crystal of 1 in 65.5% yield. Elemental analysis calcd (%) for compound **1** ($C_{36}H_{77}N_4O_{37}P_5$, formula weight: 1312.87): C 32.93; H 5.91; N 4.27; Found: C 33.02; H 5.83; N 4.19.

2.3. Single-crystal structure determination

Crystallographic data of single crystals of **1** were obtained using a Bruker AXS CCD area-detector diffractometer with Mo-Kα radiation ($\lambda = 0.71073$ Å) at 100 and 296 K. The data collection and cell refinements were obtained using the CrystalClear software package (Rigaku). The structures were solved by direct methods and successive Fourier synthesis and refined on F_2 by the full-matrix least-squares method (SHELXTL-97). All non-hydrogen atoms were refined anisotropically using reflections with $I > 2\delta$ (I). Hydrogen atoms were added geometrically and refined using the riding model with Uiso(H) = 1.2Ueq. The packing views were drawn with Crystal Make, and selected bond distances and angles were calculated using SHELXTL. Table 1 provides a summary of the crystallographic data and details of the data collection and refinement. CCDC: 1569746 (100 K) and CCDC: 1569747 (296 K) for **1** contain the supplementary crystallographic data from this study. These data can be obtained free of charge from The Cambridge Crystallographic Data Centre via www.ccdc.cam.ac.uk/data_request/cif.

2.4. Calculations

To characterize the molecular motions of the 3-nitroanilinium cation, potential energy calculations were performed at the RHF/6-31G(d) level of theory. The structural units of compound **1** used in the calculations were (3-nitroanilinium)$_3$(18-crown-6)$_3$(H_2PO_4)$_2$ and (3-nitroanilinium)$_3$(18-crown-6)$_3$, which differ from the actual stoichiometry of the compound to make the calculations computationally tractable. These computations were based on the fixed atomic coordinates obtained from the crystal structure at 296 K. The relative energy was calculated by evaluating the rigid rotation of the $C_{(25)}$–$N_{(1)}$ bond axes in 30° increments (electronic supplementary material, figure S9a). The nearest-neighbour molecules around the nitro-group (–NO_2) of the 3-nitroanilinium cation were included in the calculation of the potential energy curves (electronic supplementary material, figure S9b and S9c). The relative energy of the structure was obtained by evaluating the rigid rotation of the nitro group along the $C_{(27)}$–$N_{(2)}$ and $C_{(33)}$–$N_{(4)}$ bonds, with the rotation performed every 5° in the range of −35° to 35°.

Table 1. Crystal data and structural refinements for compound **1** at 100 and 296 K.

temperature	100 K	296 K
chemical formula	$C_{36}H_{77}N_4O_{37}P_5$	$C_{36}H_{77}N_4O_{37}P_5$
formula weight	1312.87	1312.87
crystal size (mm^3)	0.21 × 0.20 × 0.19	0.21 × 0.20 × 0.19
crystal system	monoclinic	monoclinic
space group	$P2_1/c$	$P2_1/n$
a (Å)	13.8655(17)	13.949(2)
b (Å)	25.404(3)	25.907(5)
c (Å)	21.834(3)	16.829(3)
α (°)	90.00	90.00
β (°)	129.423(9)	90.085(2)
γ (°)	90.00	90.00
V ($Å^3$)	5941.0(13)	6081.7(18)
Z	4	4
D_{calc} (g cm^{-1})	1.468	1.433
F(000)	2768	2764
m (mm^{-1})	0.255	0.249
measured 2q range (°)	0.998–25.01	0.992–25.01
R_{int}	0.0344	0.0571
R ($I > 2s(I)$)[a]	0.0401	0.1168
$_wR$ (all data)[b]	0.1029	0.1350
GOF	1.047	1.033

[a] $R = \sum(|F_o| - |F_c|) / \sum|F_a|$.
[b] $R_w^2 = \sum_w (F_o^2 - F_c^2)^2 / \sum_w (F_o^2)^2$.

3. Results and discussion

3.1. Spectral properties

The structure of compound **1** was characterized by IR spectroscopy (electronic supplementary material, figure S1). The IR spectrum of compound **1** shows a series of characteristic peaks at 1543, 1458 and 1355 cm^{-1}, which are assigned to the skeletal vibrations of the benzene rings. The strong broad peak from 2715 to 3246 cm^{-1} indicates that the $-NH_2$ group is protonated by means of intermolecular N–H···O hydrogen bonds. Characteristic peaks of the 18-crown-6 molecules are observed at 1099, 993 and 835 cm^{-1}, which we attribute to their –O-C-C- structural units. The bands within the 1051–848 cm^{-1} region are characteristic of the P-O stretching vibrations in H_3PO_4 or $H_2PO_4^-$. Overall, these results establish the existence of three constituents in compound **1** as 3-nitroanilinium, 18-crown-6, and $H_3PO_4/H_2PO_4^-$.

3.2. Differential scanning calorimetry and thermogravimetric analysis

DSC is a thermodynamic method that detects the temperature dependence of reversible phase transitions. When a compound is subjected to a disorder–order transition of molecular or proton motion, reversible heat anomalies upon heating and cooling can be detected in DSC measurements. In such measurements of **1**, a pair of reversible heat anomalies at 231/241 K (cooling/heating) was clearly observed, indicating that **1** exhibits a phase transition at $Tc = 241$ K (figure 1). The relatively large heat hysteresis of 10 K and the peak shapes indicate the occurrence of a reversible phase transition with a probable first-order feature. Entropy changes ΔS in the cooling and heating processes were estimated to be 6.32 and 8.19 J (mol K)$^{-1}$, respectively. According to Boltzmann's

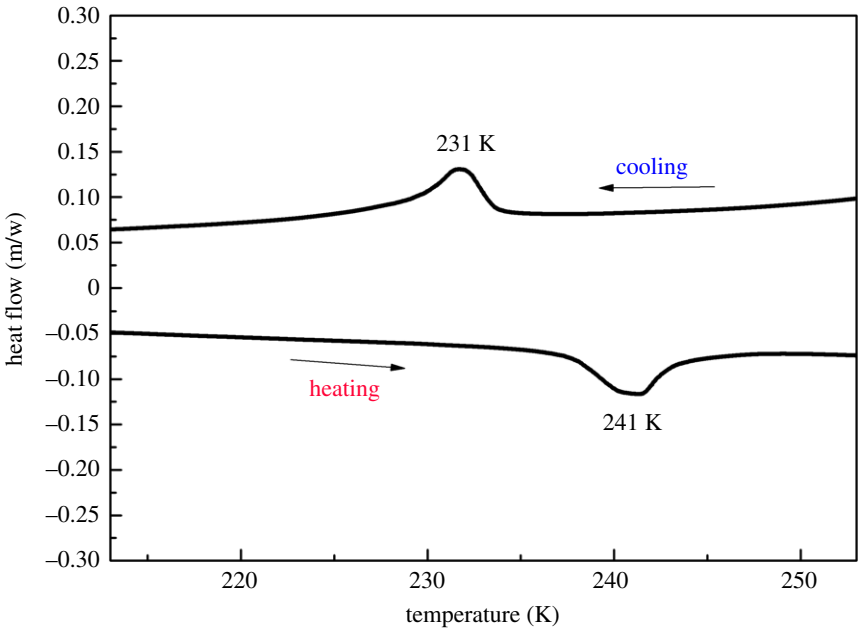

Figure 1. DSC curves of **1** obtained for heating–cooling experiments at a heating rate of 10 K min^{-1}.

equation, $\Delta S = R\ln(N)$, where R is the universal gas constant and N is the ratio of the number of geometrically distinguishable orientations, the values of N_1 and N_2 are calculated as 2.14 and 2.68, respectively. These values suggest that the number of independent orientations of disordered moieties in the crystal structure of **1** changed during the phase transition, which will be confirmed by structural analysis (vide infra).

The thermal behaviour of **1** was investigated through TG and DTA measurements from 300 to 850 K (electronic supplementary material, figure S2). The DTA curve shows a relatively weak endothermic peak at 421.5 K, which corresponds to the melting point of **1**. The TG curve reveals two main weight loss regions. The structure of compound **1** remains ordered up to 421.5 K. The first weight loss comprises approximately 61.98% of the total weight, and appears to involve the loss of (3-nitroanilinium)$_2$(18-crown-6)$_2$(H_2O) (calcd. at 63.54%). The second weight loss step of 38.02% (calcd. at 37.84%) involves three H_3PO_4 molecules and two $H_2PO_4^-$ anions.

3.3. Crystal structure of 1

The phase transition of **1** was further confirmed at 100 K (low-temperature phase, LTP) and 296 K (room-temperature phase, RTP) by variable-temperature single-crystal X-ray structure determination. The RTP structure was solved in the monoclinic $P2_1/n$ space group with cell parameters of $a = 13.949(2)$ Å, $b = 25.907(5)$ Å, $c = 16.829(3)$ Å, $\beta = 90.085(2)^\circ$, $V = 6081.7(18)$ Å^3, and $Z = 4$. The LTP structure was crystallized in the same monoclinic space group $P2_1/c$ with cell parameters of $a = 13.8655(17)$ Å, $b = 25.404(3)$ Å, $c = 21.834(3)$ Å, $\beta = 129.423(9)^\circ$, $V = 5941.0(13)$ Å^3, and $Z = 4$. By comparison of their cell parameters and refinements data, obvious changes in the c-axis and β angle in the RTP and LTP structures are evident. First, the unit cell length c extends from 16.829(3) Å to 21.834(3) Å for **1**, an increase of *ca* 23%. Second, a significant change in the β angle from 90° to 129.423° is observed. The structural anomalies corresponding to the phase transition can be ascertained by measuring the unit cell parameters of **1** as a function of temperature from 100 to 296 K (figure 2). The lattice constants along the a and b axes show small differences between the LTP and RTP as a function of temperature. The other cell parameters, c and β, exhibit an abrupt increase near 235 K, suggesting that this phase transition is of first-order nature. Notably, this result is consistent with the results of the DSC measurements.

The asymmetric unit of **1** contains two 18-crown-6 molecules, two 3-nitroanilinium cations, two $H_2PO_4^-$ anions, three H_3PO_4 molecules, and a H_2O molecule in the LTP and RTP structures (figure 3). Although the anisotropic thermal factors of all atoms in the RTP of **1** were larger than those in the LTP, no significant changes in the crystal structure are evident (electronic supplementary material, figure S3 and table S4). The 3-nitroanilinium cation interacts with the 18-crown-6 moiety by way of

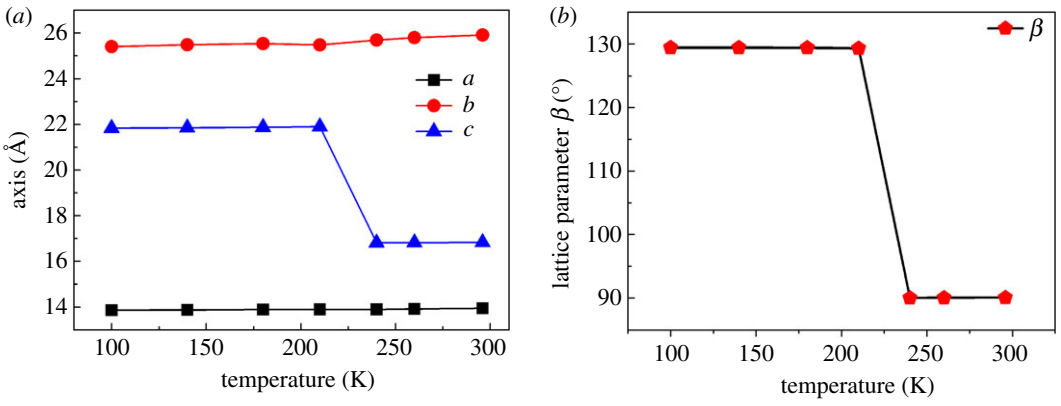

Figure 2. Temperature dependence of (*a*) cell parameters for three axis lengths and (*b*) β in the range from 100 to 296 K in **1**.

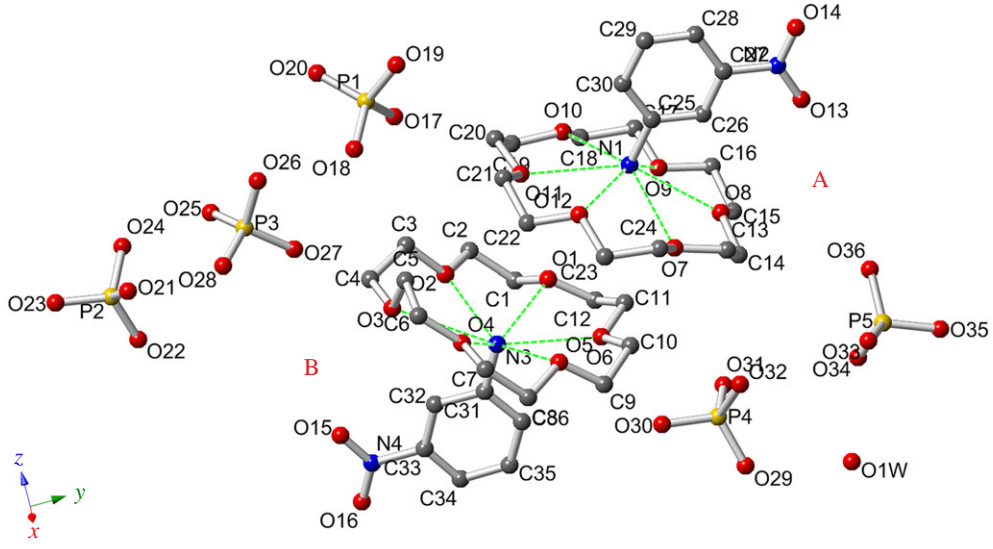

Figure 3. View of the asymmetric unit of compound **1** at 100 K with an atomic numbering scheme.

six N–H···O hydrogen bonds, thereby forming two similar supramolecular cations: (3-nitroanilinium)(18-crown-6)(A) (containing atoms N_1 and N_2) and (3-nitroanilinium)(18-crown-6)(B) (containing atoms N_3 and N_4). For convenience, we have labelled the supramolecular cation A as LTP-A and RTP-A and the supramolecular cation B as LTP-B and RTP-B in the LTP and RTP structures. In LTP-A and RTP-A, a 1 : 1 $[(3\text{-nitroanilinium})(18\text{-crown-6})]^+$ complex was formed through intermolecular $-NH_3^+\cdots O$ hydrogen-bonding interactions between the ammonium moiety of the 3-nitroanilinium cation and six oxygen atoms of the 18-crown-6 moiety. The average hydrogen-bonding distances involving N_1–O were 2.900 Å (RTP) and 2.916 Å (LTP), which are almost identical to the standard $NH_3^+\cdots O$ distance. This suggests that there was no distinct proton transfer in the N–H···O hydrogen bonds of the supramolecular cation A (electronic supplementary material, table S1). Further, the six oxygen atoms of the 18-crown-6 molecule are nearly coplanar. Indeed, the dihedral angles between the upper three (O_8, O_{10}, O_{12}) and lower three (O_7, O_9, O_{11}) oxygen planes are 1.85° at 100 K and 4.06° at 296 K, respectively. The 18-crown-6 molecules display slight distortion, with average O–C–C–O torsion angles varying from 60.38° to 68.38° in the LTP structure and from 45.15° to 68.12° in the RTP structure (electronic supplementary material, table S3).

The most notable differences in the structures of LTP-B and RTP-B occur for the dihedral angles between the nitro group and the aromatic ring of the 3-nitroanilinium cation (0.81° and 4.29°, respectively), which are similar to the analogous values of 1.93° and 4.89° in the LTP-A and RTP-A structures. This may be caused by intermolecular repulsion between the adjacent hydrogen atoms of the 3-nitroanilinium cations and $H_2PO_4^-$ anions. It is clearly shown that pendulum-like motions of the nitro group can occur easily, and such motions may be the driving force for the reversible phase

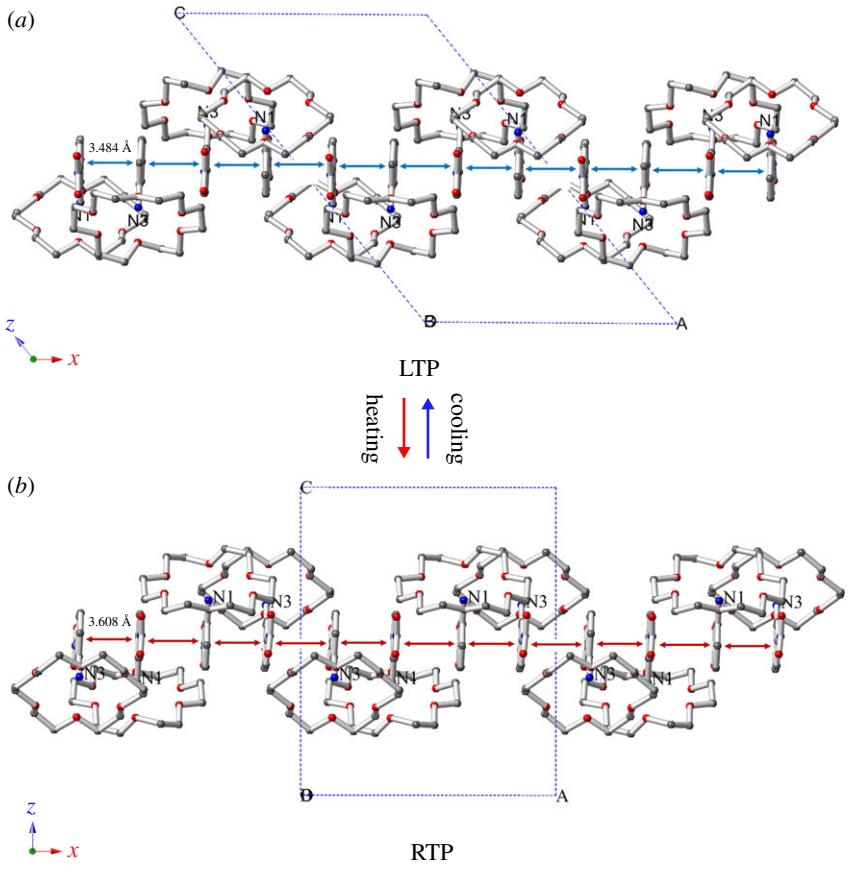

Figure 4. Crystal structure packing diagrams of supramolecular cations at (*a*) 100 K (LTP) and (*b*) 296 K (RTP) of **1** viewed along the *b*-axis. The dashed lines indicate $\pi-\pi$ interactions.

transition of **1** (electronic supplementary material, figure S5). The hydrogen bond interactions among the nitrogen and oxygen atoms include $N_3\cdots O$ bond lengths of 2.916 Å in the RTP structure and 2.903 Å in the LTP structure. The values of the N–H···O hydrogen bond distances are similar in the RTP and LTP structures, and they are consistent with that of the supramolecular cation A. At the same time, the benzene ring Cg′ (O_{25}, O_{26}, O_{27}, O_{28}, O_{29}, O_{30}, N_1, N_2) of the supramolecular cation A is connected with the neighbouring benzene ring Cg″ (O_{31}, O_{32}, O_{33}, O_{34}, O_{35}, O_{36}, N_3, N_4) of the supramolecular cation B through $\pi-\pi$ intermolecular interactions. The result of these interactions is formation of an unusually compact one-dimensional chain structure for LTP and RTP (figure 4 and electronic supplementary material, figure S6). By comparing the distances of the $\pi-\pi$ interactions in the two LTP and RTP structures, an average Cg′–Cg″ distance of 3.608 Å in the RTP structure is determined, which is slightly longer than that in the LTP structure (3.484 Å, table 2). The dihedral angles between the benzene rings in Cg′–Cg″ are 1.95° and 0.86° in the LTP and RTP structures, respectively (electronic supplementary material, figure S4). These results suggest that the 3-nitroanilinium cations move slightly along the C–N bond in the space between the supramolecular cations A and B.

According to the law of charge conservation, the inorganic anions in the non-supramolecular cation part of **1** consist of two $H_2PO_4^-$ (dihydrogen phosphate) anions, three H_3PO_4 (neutral phosphoric acid) molecules and one H_2O molecule. In the LTP and RTP structures, O–H···O hydrogen bonds were formed by two $H_2PO_4^-$ anions, three H_3PO_4 molecules and one H_2O molecule, resulting in the formation of a three-dimensional (3D) framework with one-dimensional (1D) channels (figure 5). The average O···O bond lengths are 2.558 Å (LTP) and 2.670 Å (RTP), and the O–H···O bond lengths fall in the range of 2.436–2.839 Å (LTP) and 2.519–3.169 Å (RTP). The large deviation of the O–H···O hydrogen bond distance in the three-dimensional frameworks displays a much shorter average hydrogen bond distance in the LTP structure than in the RTP structure. The change of the relative position of the $H_2PO_4^-$ anion, H_3PO_4 molecules and H_2O molecules leads to a 3D deformation of the anionic framework on going from the LTP structure to the RTP one, causing the protons to move more easily within the O–H···O hydrogen-bonding network. In the crystal packing structure,

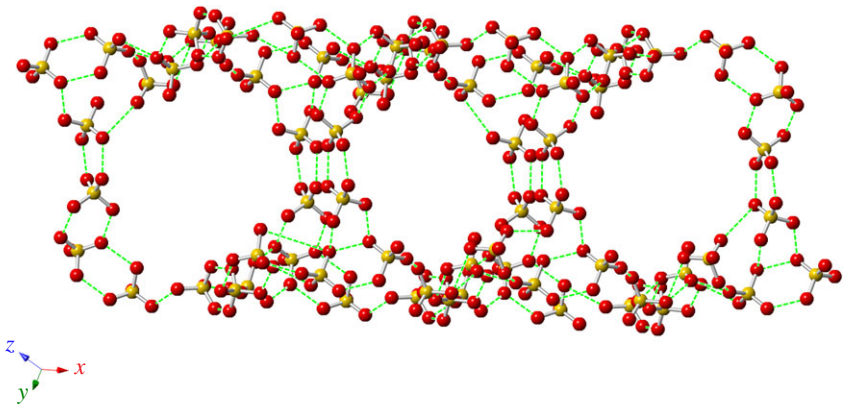

Figure 5. View of the 3D framework packing of the $H_2PO_4^-$ anions and H_3PO_4 and H_2O molecules by O–H···O hydrogen-bonding interactions. The dashed lines indicate hydrogen bonds.

Table 2. Dihedral angles and average Cg′ and Cg″ distances with $\pi-\pi$ interactions along the *a*-axis at 100 and 296 K.

angle (°)	∠Cg′ – Cg″	∠Cg″ – Cg″	∠Cg″ – Cg′	∠Cg′ – Cg′
100 K	1.95	0.00	1.95	0.00
296 K	0.86	0.00	0.86	0.00
distance (Å)	d(Cg′ – Cg″)	d(Cg″ – Cg″)	d(Cg″ – Cg′)	d(Cg′ – Cg′)
100 K	3.484	3.580	3.484	3.544
296 K	3.663	3.627	3.552	3.609

independent supramolecular cations are located in the 1D channels through $\pi-\pi$ intermolecular interactions and insert into the cavities of the 3D framework by O–H···O hydrogen bonds (figure 6; electronic supplementary material, figures S7 and S8). As shown in figure 7, we measured the size of the cavity in the direction of the *b*-axis; it is 20.965 Å in the RTP structure, which is slightly longer than that in the LTP structure (19.619 Å). Meanwhile, the cavity sizes in the direction of the equatorial plane are 15.911 Å in the LTP structure and 16.803 Å in the RTP structure. Hence, the relatively small cavity reduces the extent of pendulum-like rotational motion of the nitro group of the 3-nitroanilinium cation.

3.4. Potential energy calculations

To confirm whether the motions of the 3-nitroanilinium cations and nitro groups make significant contributions to the phase transitions, the potential energies for (i) rotation of the phenyl ring and (ii) pendulum-like motion of the nitro group were calculated with the RHF/6-31(d) level of theory. These calculations were based on the fixed atomic coordinates obtained from the crystal structure at 296 K. The model used for these calculations is shown in electronic supplementary material, figure S9a. For the phenyl ring motion along the C_{25}–N_1 axis, the atomic coordinates of the $-NH_3^+$ groups were kept fixed while rigid motion of the phenyl ring was applied to calculate the rotational potential energy. Three 18-crown-6 molecules, two 3-nitroanilinium cations, and two $H_2PO_4^-$ anions were included in the models to evaluate the effects of steric hindrance. The rotational angle (Φ) dependencies of the potential energies (ΔE) for the phenyl ring in compound **1** from 0° to 360° at 30° increments are provided in figure 8*a*. The initial atomic coordinates obtained from the crystal structure at 296 K correspond to the first potential energy minimum at $\Phi = 0°$, whose relative energy was defined as zero. The second and third potential energy minima appear at $\Phi = 120°$ and 240°, respectively, for the phenyl ring in **1**, and the maxima were calculated at $\Phi = 90°$, 180° and 270°, with corresponding ΔE values of 965.90, 993.05 and 958.24 kJ mol^{-1}, respectively. The magnitude of the maximum ΔE for the phenyl ring (≈1000 kJ mol^{-1}) was far greater than that in (m-fluoroanilinium$^+$)(DB[18]-crown-6)[Ni(dmit)$_2$]$^-$(≈270 kJ mol^{-1}) [8]. The high potential energy barriers for rotation of the phenyl ring suggest that it is almost impossible above room temperature.

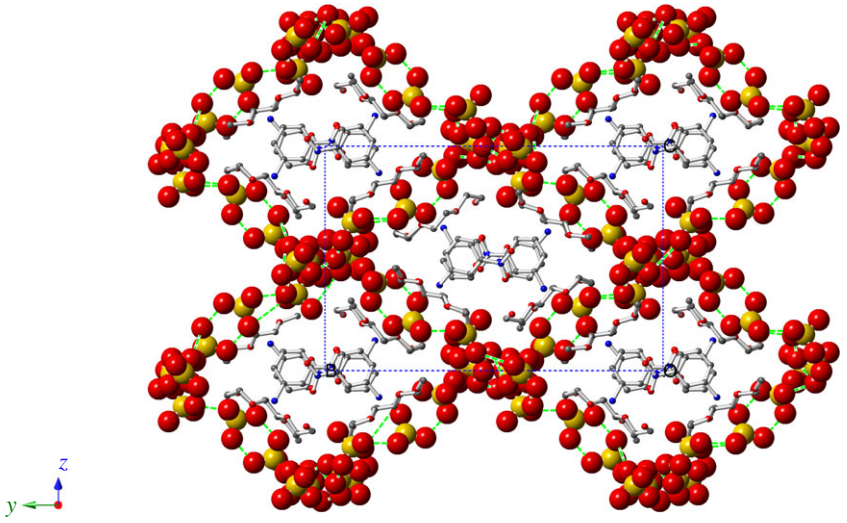

Figure 6. Crystal packing of **1** along the *a*-axis. The independent supramolecular cations are located in the 1D channels through $\pi-\pi$ intermolecular interactions and insert into the cavity of the 3D framework by O–H···O hydrogen bonds.

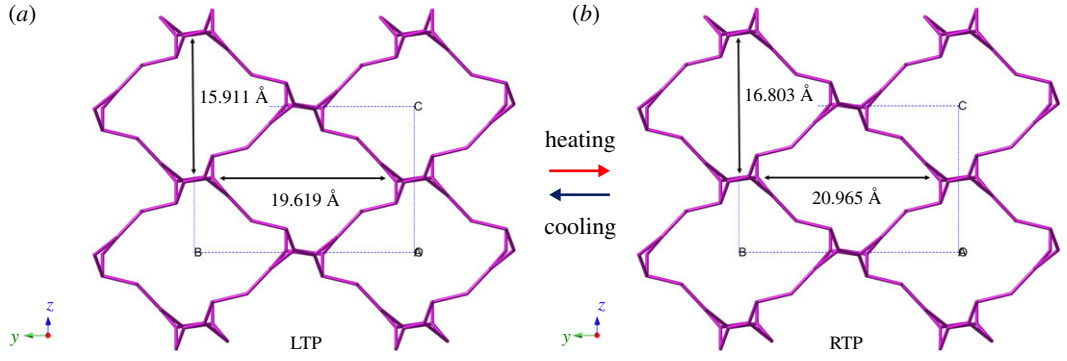

Figure 7. Schematic model of the 3D framework at (*a*) 100 K (LTP) and (*b*) 296 K (RTP). The solid lines indicate the conformational changes viewed along the *b*- and *c*-axes.

The pendulum-like motion of the nitro group was evaluated with fixed atomic coordinates of the C_6H_4–NO_2 moiety in the supramolecular cations. The models used for these calculations comprise three supramolecular cations $[(3\text{-nitroanilinium})(18\text{-crown-6})]^+$ (electronic supplementary material, figure S9b and S9c). Because rotation of the nitro group by 360° is very likely to be impossible because of the large steric hindrance of the neighbouring phenyl rings, the relative energy of pendulum-like motion of the nitro group was calculated at 5° increments within the range of −35° to 35°. Two symmetrical potential energy profiles were calculated for this motion in the supramolecular cations A and B (figure 8*b*). The magnitude of the maximum ΔE was *ca* 140 kJ mol^{-1} (less than 270 kJ mol^{-1}), indicating that pendulum-like motion of the nitro group around the C_{27}–N_2 and C_{33}–N_4 bonds is possible at 296 K. Consequently, such motion is likely to be restricted at 100 K but easily activated as the temperature is increased. Overall, these results suggest that the pendulum-like motion of the nitro group may well be related to the observed phase transitions.

3.5. Dielectric properties

It is well known that physical properties usually display abrupt changes in the vicinity of a phase transition, and the magnitude is correlated to characteristic features of the phase transition. The dielectric properties of **1** were measured in three directions of a single-crystal sample. The temperature dependence of the real parts (ε') of the dielectric constants taken at 5 kHz, 10 kHz, 100 kHz and 1 MHz are depicted in figure 9 and electronic supplementary material, figure S10. The T–ε' curve shows two obvious step-like dielectric anomalies in the temperature range of 150–280 K, which is consistent with the results determined using DSC. At 5 kHz, ε' remains at approximately 11–12 from

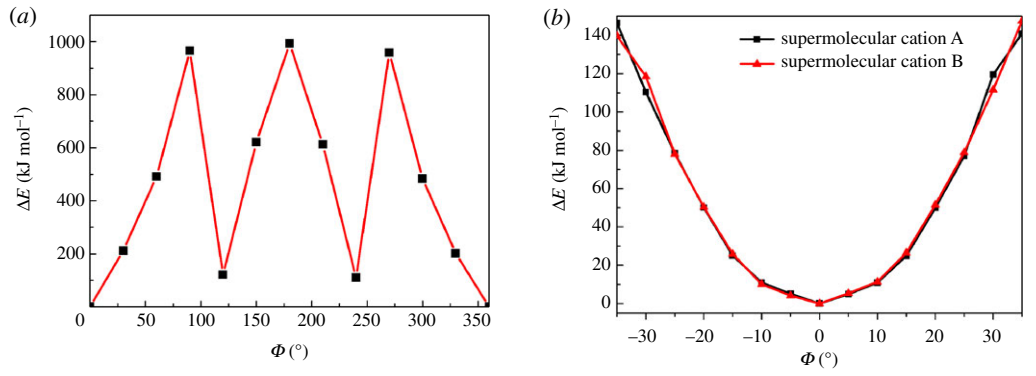

Figure 8. Potential energy curves for (*a*) rotational motion of the phenyl ring of the 3-nitroanilinium cation along its C–N bond and (*b*) pendulum-like motion of the nitro group in the range of −35° to 35°.

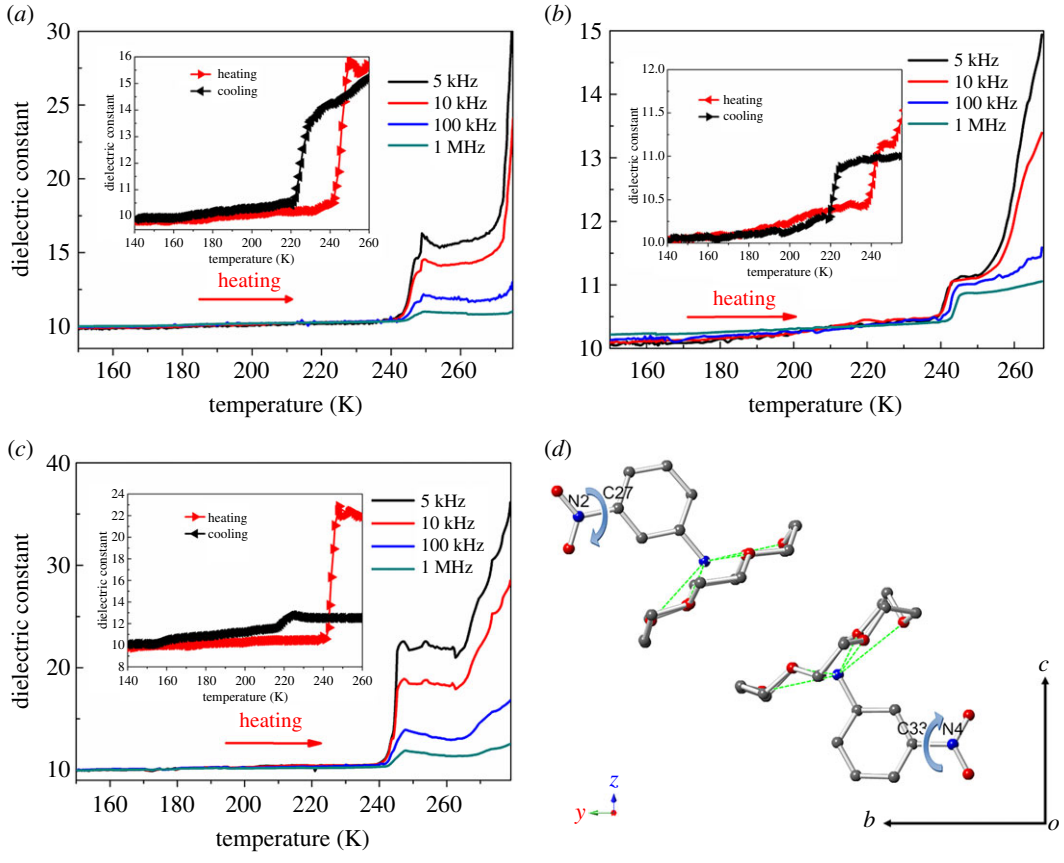

Figure 9. Anisotropic dielectric constants of **1** along (*a*) *a*-, (*b*) *b*- and (*c*) *c*-axes at 5 kHz to 1 MHz upon heating. (*d*) The pendulum-like motion of the nitro-group in supramolecular cations A and B corresponds to the direction of the *ac*-plane. Insert: the thermal hysteresis curves at 5 kHz.

150 to 242 K; it then increases to a maximum of approximately 17 at *ca* 250 K along the *a*-axis (figure 9*a*). Figure 9*b* and electronic supplementary material, figure S10b display two clear step-like dielectric anomalies at approximately 225 K on cooling and 242 K on heating. For the *c*-axis, two step-like dielectric anomalies similar to that observed for the *a*- and *b*-axes were also observed (figure 9*c* and electronic supplementary material, figure S10c). In the heating mode, ε' remains stable (approx. 10) until the temperature reaches *ca* 242 K at different frequencies, corresponding to the low dielectric state. With rising temperature, the ε' exhibited a prominent increase from *ca* 10 to 25, 20, 14, and 12 at 5 kHz, 10 kHz, 100 kHz, and 1 MHz, respectively. Upon cooling again, the curves plateau with a slight decrease and the ε' values change from *ca* 12.8 to 11.8 at a frequency of 5 kHz. The changes of

ε' at lower frequencies are more pronounced than those at higher frequencies, indicating that the dielectric constant is very sensitive to external frequencies. From analysis of the crystal structure of **1**, the dielectric anisotropy was related to the anisotropy of proton transfer in the 3D framework through O–H···O hydrogen bonds. In addition, the temperature-dependent curves of ε' along the *a*-, *b*- and *c*-axes obtained in the cooling mode match well with those obtained during the heating process, suggesting the occurrence of a reversible phase transition.

Distinct step-like anomalies around 241 K can be viewed along both the *a*- and *c*-axes, while relatively smaller anomalies are apparent along the *b*-axis. These phenomena can be explained by examining the dynamic motion of the nitro group in the cation. Pendulum-like motion of this group occurs in the *ac*-plane, which enhances the ε' along the *a*- and *c*-axes. The fluxional frequency of the nitro group motion coupling with proton transfer is suppressed as the temperature decreases, when they become frozen in a given state. Therefore, there is no obvious change in the value of ε' with changing frequency; it does increase with increasing temperature, however. Further dielectric enhancement was observed at temperatures above 260 K, where the low-frequency and ε' was larger than the high-frequency values. Importantly, the phase transition of compound **1**, which can be tuned between low and high dielectric states at low and room temperature, makes it an excellent candidate for molecular switchable dielectrics.

4. Conclusion

In conclusion, a new three-dimensional organic–inorganic hybrid compound, (3-nitroanilinium)$_2$(18-crown-6)$_2$(H_2PO_4)$_2$(H_3PO_4)$_3$(H_2O) (**1**), was synthesized. Compound **1** undergoes a reversible phase transition at *ca* 231 K, which is anisotropy in the vicinity of *T*c. The dynamic behaviours between the pendulum-like motions of the nitro group in the organic cations and proton transfer in the O–H···O hydrogen bonds of the 3D framework produce a synergistic effect that gives rise to the observed phase transition and distinct dielectric anisotropy along various crystallographic axes. Notably, the dielectric constants could be switched by continuous phase transitions and tuned in the low and high dielectric states, indicating the potential application of structures like **1** in switchable dielectrics. We believe that this example will inspire new strategies for the successful design of other organic–inorganic hybrid multifunctional materials.

Ethics. We were not required to complete an ethical assessment before conducting the research. No data were collected from human or animal subjects for the purpose of this study.

Data accessibility. This article does not contain any additional data.

Authors' contributions. Z.-q.L. designed the method and wrote the manuscript; X.-y.Z. synthesized the crystal materials. Y.L. and C.-l.Z. supported the dielectric constant and DSC measurements. L.-l.Q. and S.-x.Y. analysed the crystal data of **1**. All authors have given approval the final version of the paper.

Competing interests. There are no conflicts of interest to declare.

Funding. The present work was supported by the National Natural Science Foundation of China (no. 21561030) (Z.-q.L.), Program for High-Level Talents Introduction of Xinjiang Uygur Autonomous Region (Z.-q.L.), and '1000 Talent Plan' on Overseas High-Level Talents Introduction (CCCPC) (Z.-q.L.).

References

1. Fu H, Cohen RE. 2000 Polarization rotation mechanism for ultrahigh electromechanical response in single-crystal piezoelectrics. *Nature* **403**, 281–283. (doi:10.1038/35002022)
2. Fu DW, Cai HL, Liu Y, Ye Q, Zhang W, Zhang Y, Chen XY, Giovannetti G, Capone M, Li J, Xiong RG. 2013 Diisopropylammonium bromide is a high-temperature molecular ferroelectric crystal. *Science* 339, 425–428. (doi:10.1126/science.1229675)
3. Horiuchi S, Tokunaga Y, Giovannetti G, Picozzi S, Itoh H, Shimano R, Kumai R, Tokura Y. 2010 Above-room-temperature ferroelectricity in a single-component molecular crystal. *Nature* **463**, 789–793. (doi:10.1038/nature08731)
4. You Y-M, Tang Y-Y, Li P-F, Zhang H-Y, Zhang W-Y, Zhang Y, Ye H-Y, Nakamura T, Xiong R-G. 2017 Quinuclidinium salt ferroelectric thin-film with duodecuple-rotational polarization-directions. *Nat. Commun.* **8**, 14934. (doi:10.1038/ncomms14934)
5. Hang T, Zhang W, Ye H-Y, Xiong R-G. 2011 Metal-organic complex ferroelectrics. *Chem. Soc. Rev.* **40**, 3577–3598. (doi:10.1039/c0cs00226g)
6. Zhao W-P, Jin Y, Zhang W. 2016 Phase transitions in two organic salts based on 1,5-naphthalenedisulfonate. *Sci. China Chem.* **59**, 114–121. (doi:10.1007/s11426-015-5442-6)
7. Li L-N *et al.* 2018 Bilayered hybrid perovskite ferroelectric with giant two-photon absorption. *J. Am. Chem. Soc.* **140**, 6806–6809. (doi:10.1021/jacs.8b04014)
8. Sun Z-H, Li J, Ji C-M, Sun J-L, Hong M-C, Luo J-H. 2017 Unusual long-range ordering incommensurate structural modulations in an organic molecular ferroelectric. *J. Am. Chem. Soc.* **139**, 15 900–15 906. (doi:10.1021/jacs.7b08950)
9. Li L-N, Sun Z-H, Wang P, Hu W-D, Wang S-S, Ji C-M, Hong M-C, Luo J-H. 2017 Tailored engineering of an unusual ($C_4H_9NH_3$)$_2$(CH_3NH_3)$_2$$Pb_3Br10$ two-dimensional multilayered perovskite ferroelectric for a high-performance photodetector. *Angew. Chem. Int. Ed.* **56**, 12 150–12 154. (doi:10.1002/anie.201705836)

10. Horiuchi S, Ishii F, Kumai R, Okimoto Y, Tachibana H, Nagaosa N, Tokura Y. 2005 Ferroelectricity near room temperature in co-crystals of nonpolar organic molecules. *Nat. Mater.* **4**, 163–166. (doi:10.1038/nmat1298)
11. Akutagawa T, Koshinaka H, Sato D, Takeda S, Noro S-I, Takahashi H, Kumai R, Tokura Y, Nakamura T. 2009 Ferroelectricity and polarity control in solid-state flip-flop supramolecular rotators. *Nat. Mater.* **8**, 342–347. (doi:10.1038/nmat2377)
12. Akutagawa T, Takeda S, Hasegawa T, Nakamura T. 2004 Proton transfer and a dielectric phase transition in the molecular conductor $(HDABCO^+)_2(TCNQ)_3$. *J. Am. Chem. Soc.* **126**. 291–294. (doi:10.1021/ja0377697)
13. Zhang W, Ye H-Y, Cai H-L, Ge J-Z, Xiong R-G, Huang S-D. 2010 Discovery of new ferroelectrics: $[H_2dbco]_2$·$[Cl_3]$·$[CuCl_3(H_2O)_2]$·H_2O (dbco = 1,4-diazabicyclo[2.2.2]octane). *J. Am. Chem. Soc.* **132**, 7300–7302. (doi:10.1021/ja102573h)
14. Sun Z-H, Liu X-T, Khan T-K, Ji C-M, Asghar M-A, Zhao S-G, Li L-N, Hong M-C, Luo J-H. 2016 A photoferroelectric perovskite-type organometallic halide with exceptional anisotropy of bulk photovoltaic effects. *Angew. Chem. Int. Ed.* **55**, 6545–6550. (doi:10.1002/anie.201601933)
15. Sun Z-H, Tang Y-Y, Zhang S-Q, Ji C-M, Chen T-L, Hong M-C, Luo J-H. 2015 Ultrahigh pyroelectric figures of merit associated with distinct bistable dielectric phase transition in a new molecular compound: di-n-butylaminium trifluoroacetate. *Adv. Mater.* **27**, 4795–4801. (doi:10.1002/adma.201501923)
16. Ye H-Y, Ge J-Z, Tang Y-Y, Li P-F, Zhang Y, You Y-M. 2016 Molecular ferroelectric with most equivalent polarization directions induced by the plastic phase transition. *J. Am. Chem. Soc.* **138**, 13 175–13 178. (doi:10.1021/jacs.6b08817)
17. Liu Z-Q, Kubo K, Lin L, Hoshino N, Noro S-I, Akutagawa T, Nakamura T. 2013 Molecular motion in pyridazinium/crown ether supramolecular cation salts of a nickel dithiolene complex. *Dalton Trans.* **42**, 2930–2939. (doi:10.1039/c2dt32542j)
18. Wang Z-X, Liao W-Q, Ye H-Y, Zhang Y. 2015 Sequential structural transitions with distinct dielectric responses in a layered perovskite organic-inorganic hybrid material: $[C_4H_9N]_2[PbBr_4]$. *Dalton Trans.* **44**, 20 406–20 412. (doi:10.1039/C5DT03277F)
19. Mao C-Y, Liao W-Q, Wang Z-X, Li P-F, Lv X-H, Ye H-Y, Zhang Y. 2016 Structural characterization, phase transition and switchable dielectric behaviors in a new zigzag chain organic-inorganic hybrid compound: $[C_3H_7NH_3]_2SbI_5$. *Dalton Trans.* **45**, 5229–5233. (doi:10.1039/C5DT04939C)
20. Xu W-J, Li P-F, Tang Y-Y, Zhang W-X, Xiong R-G, Chen X-M. 2017 A molecular perovskite with switchable coordination bonds for high-temperature multi-axial ferroelectrics. *J. Am. Chem. Soc.* **139**, 6369–6375. (doi:10.1021/jacs.7b01334)
21. Tang Y-Z, Gu Z-F, Xiong J-B, Gao J-X, Liu Y, Wang B, Tan Y-H, Xu Q. 2016 Unusual sequential reversible phase transitions containing switchable dielectric behaviors in cyclopentyl ammonium 18-crown-6 perchlorate. *Chem. Mater.* **28**, 4476–4483. (doi:10.1021/acs.chemmater.6b01726)
22. Ye H-Y, Li S-H., Zhang Y, Zhou L, Deng Fa, Xiong R-G. 2014 Solid state molecular dynamic investigation of an inclusion ferroelectric: [(2,6-diisopropylanilinium)([18]crown-6)]BF_4. *J. Am. Chem. Soc.* **136**, 10 033–10 040. (doi:10.1021/ja503344b)
23. Li Q, Shi P-P, Ye Q, Wang H-T, Wu D-H, Ye H-Y, Fu D-W, Zhang Y. 2015 A switchable molecular dielectric with two sequential reversible phase transitions: $[(CH_3)_4P]_4[Mn(SCN)_6]$. *Inorg. Chem.* **54**, 10 642–10 647. (doi:10.1021/acs.inorgchem.5b01437)
24. Liu Z-Q, Kubo K, Noro S-I, Akutagawa T, Nakamura T. 2014 Design of crystalline spaces for molecular rotations in crystals. *Cryst. Growth Des.* **14**, 537–543. (doi:10.1021/cg4013262)
25. Lv X-H, Liao W-Q, Wang Z-X, Li P-F, Mao C-Y, Ye H-Y. 2016 Design and prominent dielectric properties of a layered phase-transition crystal: $(cyclohexylmethylammonium)_2CdCl_4$. *Cryst. Growth Des.* **16**, 3912–3916. (doi:10.1021/acs.cgd.6b00480)
26. Zhang Y, Ye H-Y, Fu D-W, Xiong R-G. 2014 An order-disorder ferroelectric host-guest inclusion compound. *Angew. Chem. Int. Ed.* **53**, 2114–2118. (doi:10.1002/anie.201307690)
27. Wang W-X, Zhu R-Q, Fu X-Q, Zhang W. 2012 Crystal structure and dielectric property of $(p\text{-}CH_3OC_6H_4NH_3)^+$(18-crown-6)·$H_2PO_4^-$·$2H_3PO_4$. *Z. Anorg. Allg. Chem.* **638**, 1123–1126. (doi:10.1002/zaac.201200072)
28. Liu Z-Q, Liu Y, Chen Y, Zhao W-Q, Fang W-N. 2017 Synthesis, characterization, and phase transition of an inorganic-organic hybrid compound, [(3-nitroanilinium$^+$)(18-crown-6)][IO_4^-](CH_3OH). *Chin. Chem. Lett.* **28**, 297–301. (doi:10.1016/j.cclet.2016.07.013)
29. Willey G, Spry M, Errington W. 2000 Crown ether complexation of Te(IV): formation and crystal structure of [(18-crown-6)Te(Cl)(μ-$O)_2$Te(Cl)(18-crown-6)][$SbCl_6$]$_2$. *Polyhedron* **19**, 1799–1802. (doi:10.1016/S0277-5387(00)00452-6)
30. Shi P-P, Ye Q, Li Q, Wang H-T, Fu D-W, Zhang Y, Xiong R-G. 2014 Novel phase-transition materials coupled with switchable dielectric, magnetic, and optical properties: $[(CH_3)_4P][FeCl_4]$ and $[(CH_3)_4P][FeBr_4]$. *Chem. Mater.* **26**, 6042–6049. (doi:10.1021/cm503003f)
31. Ge J-Z, Fu X-Q, Hang T, Ye Q, Xiong R-G. 2010 Reversible phase transition of the 1:1 complexes of 18-crown-6 with 4-ethoxyanilinium perchlorate. *Cryst. Growth Des.* **10**, 3632–3637. (doi:10.1021/cg100523b)
32. Wang F-F, Chen C, Zhang Y, Fu D-W. 2015 Crystal structure and dielectric property of supramolecular macrocyclic [(NDPA).(18-crown-6)]$^{2+}$·$(DMA)^+$·$3ClO_4^-$ assemblies. *Chin. Chem. Lett.* **26**, 31–35. (doi:10.1016/j.cclet.2014.10.005)
33. Li P-F, Liao W-Q, Zhou Q-Q, Ye H-Y, Zhang Y. 2015 Inorganic anion regulated phase transition in a supramolecular adduct: 4-trifluoromethoxyanilinium hexafluorophosphate-18-crown-6. *Inorg. Chem. Commun.* **61**, 77–81. (doi:10.1016/j.inoche.2015.08.027)
34. Ye Q, Wang H-T, Zhou L, Kong L-H, Ye H-Y, Fu D-W, Zhang Y. 2016 Phase transition metal-crown ether coordination compounds tuned by metal ions. *Dalton Trans.* **45**, 1000–1006. (doi:10.1039/C5DT02631H)
35. Horiuchi S, Kunmai R, Tokura Y. 2007 A supramolecular ferroelectric realized by collective proton transfer. *Angew. Chem. Int. Ed.* **46**, 3497–3501. (doi:10.1002/anie.200700407)
36. Chen L-Z, Zhao H, Ge J-Z, Xiong R-G, Hu H-W. 2009 Observation of deuteration effect in co-crystal system: hexamethylenetetraminium 3,5-dinitrobenzoate hemideuterated water. *Cryst. Growth Des.* **9**, 3828–3831. (doi:10.1021/cg900348x)
37. Sun Z-H, Chen T-L, Luo J-H, Hong M-C. 2012 Bis(imidazolium) L-tartrate: a hydrogen-bonded displacive-type molecular ferroelectric material. *Angew. Chem. Int. Ed.* **51**, 3871–3876. (doi:10.1002/anie.201200407)
38. Shang R, Xu G-C, Wang Z-M, Gao S. 2014 Phase transitions, prominent dielectric anomalies, and negative thermal expansion in three high thermally stable ammonium magnesium-formate frameworks. *Chem. Eur. J.* **20**, 1146–1158. (doi:10.1002/chem.201303425)
39. Li S-G, Luo J-H, Sun Z-H, Zhang S-Q, Li L-N, Shi X-J, Hong M-C. 2013 Phase transition triggered by ordering of unique pendulum-like motions in a supramolecular complex: potassium hydrogen bis(dichloroacetate)-18-crown-6. *Cryst. Growth Des.* **13**, 2675–2679. (doi:10.1021/cg4004565)
40. Ye H-Y, Chen L-Z, Xiong R-G. 2010 Reversible phase transition of pyridinium-3-carboxylic acid perchlorate. *Acta Cryst.* **B66**, 387–395. (doi:10.1107/S0108768110001576)
41. Fu D-W, Zhao M-M, Ge J-Z. 2011 Synthesis, structure and dielectric property of two H-bonded supramolecular compounds with 1-aminoadamantane based on 18-crown-6. *J. Mol. Struct.* **1006**, 227–233. (doi:10.1016/j.molstruc.2011.09.013)
42. Ye Q, Akutagewa T, Endo T, Noro S-I, Nakamura T, Xiong RG. 2010 Asymmetrical $[Ni(dmit)_2]^-$ arrangements induced by (1R,2R)-cyclohexanediammonium—crown ether supramolecules. *Inorg. Chem.* **49**, 8591–8600. (doi:10.1021/ic101253g)
43. Tang Y-Z, Gu Z-F, Yang C-S, Wang B, Tan Y-H, Wen H-R. 2016 Unusual two-step switchable dielectric behaviors and ferroelastic phase transition in a simple 18-crown-6 clathrate. *ChemistrySelect* **1**, 6772–6776. (doi:10.1002/slct.201601860)
44. Williams N, Hancock R, Riebenspies J, Fernandes M, Sousa A-S. 2009 Complexation of mercury(I) and mercury(II) by 18-crown-6: hydrothermal synthesis of the mercuric nitrite complex. *Inorg. Chem.* **48**, 11 724–11 733. (doi:10.1021/ic9017618)
45. Luo M-B, Xiong Y-Y, Wu H-Q, Feng X-F, Li J-Q, Luo F. 2017 The MOF^+ technique: a significant synergic effect enables high performance chromate removal. *Angew. Chem. Int. Ed.* **56**, 16 376–16 379. (doi:10.1002/anie.201709197)
46. Fan C-B *et al.* 2017 Significant enhancement of C_2H_2/C_2H_4 separation by a photochromic

diarylethene unit: a temperature- and light-responsive separation switch. *Angew. Chem. Int. Ed.* **56**, 7900–7906. (doi:10.1002/anie.201702484)

47. Ye Q, Akutagawa T, Ye H-Y, Hang T, Ge J-Z, Xiong R-G, Noro S-I, Nakamura T. 2011 Structural phase transition due to the flexible supramolecule of (4-cyanomethylanilinium) ([18]crown-6) in $[Ni(dmit)_2]^-$ crystal. *CrystEngComm* **13**, 6185–6191. (doi:10.1039/C1CE05581J)
48. Mu R, Chen C-H, Zhang L, Jia D-Z, Xu G-C. 2017 Phase transition originating from disorder-order transformation coupled with reorientation in organic-inorganic hybrid material: $(C_4H_{14}N_2)[Cd_2(H_2O)_6(SO_4)_3]$. *Eur. J. Inorg. Chem.* **2017**, 932–937. (doi:10.1002/ejic.201601357)
49. Zhang Y, Zhang W, Li S-H, Ye Q, Cai H-L, Deng F, Xiong R-G, Huang S-D. 2012 Ferroelectricity induced by ordering of twisting motion in a molecular rotor. *J. Am. Chem. Soc.* **134**, 11 044–11 049. (doi:10.1021/ja3047427)
50. Tang Y-Z, Yu Y-M, Xiong J-B, Tan Y-H, Wen H-R. 2015 Unusual high temperature reversible phase transition behavior, structures and dielectric-ferroelectric properties of two new crown ether clathrates. *J. Am. Chem. Soc.* **137**, 13 345–13 351. (doi:10.1021/jacs.5b08061)
51. Wang H-T, Kong L-H, Shi P-P, Li Q, Ye Q, Fu D-W. 2015 The structure and dielectric properties of ionic compounds with flexible ammonium moiety. *Chin. Chem. Lett.* **26**, 382–386. (doi:10.1016/j.cclet.2014.10.025)
52. Nagata H, Nishi H, Kamigauchi M, Ishida T. 2006 Structural scaffold of 18-crown-6 tetracarboxylic acid for optical resolution of chiral amino acid: X-ray crystal analyses of complexes of D- and L-isomers of serine and glutamic acid. *Chem. Pharm. Bull.* **54**, 452–457. (doi:10.1248/cpb.54.452)
53. Ye Q, Shi P-P, Chen Z-Q, Akutagawa T, Noro S-I, Nakamura T. 2012 Flexible cis-cyclohexane-1,4-diammonium ion in magnetic $[Ni(dmit)_2]$ crystals. *Eur. J. Inorg. Chem.* **2012**, 3732–3739. (doi:10.1002/ejic.201200099)
54. Liu S-J, Li J, Sun Z-H, Ji C-M, Li L-N, Zhao S-G, Luo J-H. 2016. Order-disorder phase transition, anisotropic and switchable dielectric constants induced by freeze of the wheel-like motion in a hexafluorosilicate-based crystal. *ChemistrySelect* **1**, 5310–5315. (doi:10.1002/slct.201601263)
55. Liu Y, Chen Y, Xu M-J, Zhu C-L, Liu Z-Q. 2017 Synthesis, structure, and phase transition of a novel proton transfer in a supramolecular cation with 2-nitroanilinium based on 18-crown-6. *J. Mol. Struct.* **1148**, 429–434. (doi:10.1016/j.molstruc.2017.07.078)